Journal of Zhejiang University-SCIENCE A (Applied Physics & Engineering)
ISSN 1673-565X (Print); ISSN 1862-1775 (Online)
www.zju.edu.cn/jzus; www.springerlink.com
E-mail: jzus@zju.edu.cn

Geometry of screw compressor rotors and their tools#

Nikola STOSIC†, Ian K. SMITH, Ahmed KOVACEVIC, Elvedin MUJIC
(*Centre for Positive Displacement Compressors, City University London, London EC1V 0HB, UK*)
†E-mail: n.stosic@city.ac.uk

Received Sept. 4, 2010; Revision accepted Jan. 21, 2011; Crosschecked Feb. 27, 2011

Abstract: This paper presents a method of general geometrical definitions of screw machine rotors and their manufacturing tools. It describes the details of lobe shape specification, and focuses on a new lobe profile, which yields a larger cross-sectional area and shorter sealing lines resulting in higher delivery rates for the same tip speed. A well proven mathematical model was used to determine the optimum profile, compressor housing size, and compressor ports to achieve the superior compressors.

Key words: Geometry of screw compressors, Rotor lobe profile, Cutting tools
doi:10.1631/jzus.A1000393 **Document code:** A **CLC number:** TH45

1 Introduction

Screw compressor is a common type of machine used to compress gases. It consists of a pair of meshing rotors with helical grooves machined in them contained in a housing, which fits closely around them. The rotors and housing are separated by very small clearances. The rotors mesh like gears in such a manner that as they rotate the space formed between them and the housing is reduced progressively. Thus any gas trapped in this space is compressed.

Although the principles of operation of helical screw compressors have been well known for more than 120 years, it is only during the past 40 years that they have become widely used. The main reasons for that were their poor efficiency and the high cost of manufacturing their rotors. Two main developments led to a solution to these difficulties. The first was the introduction of the asymmetric rotor profile approximately 35 years ago which substantially reduced the blow-hole area, which was the main source of internal leakage, and thereby raised the thermodynamic efficiency of these machines to roughly the same level as that of traditional reciprocating compressors. The second was the introduction of precise thread milling machine tools at approximately the same time which made it possible to manufacture accurately and economically items of complex shape, such as the rotors.

From then on, as a result of their ever improving efficiencies, high reliability, and compact form, screw compressors have taken an increasing share of the compressor market, especially in the fields of compressed air production, and refrigeration and air conditioning, and today, a good proportion of compressors manufactured for industry are of this type.

As pointed out by Fleming *et al*. (1998), screw machines represent a success story of the 20th century. The main reasons for that are the development of novel rotor profiles, which have drastically reduced internal leakage, and advanced machine tools, which can manufacture the most complex shapes to tolerances of 3 mm at an acceptable cost (Holmes and Stephen, 1999). Rotor profile enhancement is still the most promising means of further improving screw compressors, and rational procedures are now being developed both to replace earlier empirically derived shapes and also to vary the proportions of the selected profile to obtain the best result for the application.

This paper is the extension on the paper of "Geometry of Screw Compressor Rotors and Their Tools", which appeared in the Proceedings of International Conference on Compressor and Refrigeration, Xi'an, China, Sept. 25-28, 2008

A screw machine volume is defined by the rotor profile, and port shape and size. The gearing algorithm used for the rotor profiling demonstrates the meshing condition, which enables a variety of rotor primary curves to be defined either analytically or by discrete points. The most efficient contemporary profiles were obtained from a combined rotor-rack generation procedure.

Screw compressor consists essentially of a pair of meshing helical lobed rotors, which rotate within a fixed housing that totally encloses them, as shown in Fig. 1. The space between any two successive lobes of each rotor and its surrounding housing forms a separate working chamber. The volume of this chamber varies as rotation proceeds due to displacement of the line of contact between the two rotors. It is a maximum when the entire length between the lobes is unobstructed by meshing contact with the other rotor. It has a minimum value of zero when there is a full meshing contact with the second rotor at the end face. The two meshing rotors effectively form a pair of helical gear wheels with their lobes acting as teeth. These are normally described as the male or main rotor and the female or gate rotor, respectively.

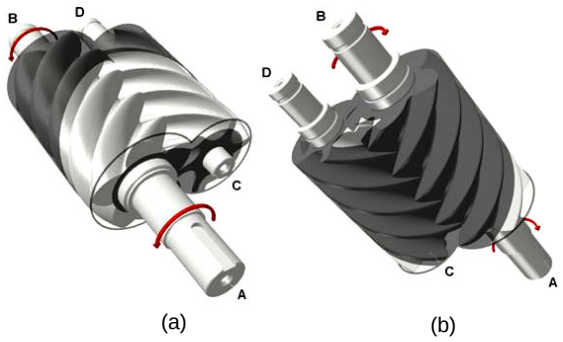

Fig. 1 Screw compressor rotors
(a) View from front and top; (b) View from bottom and rear

As shown in Fig. 1a, gas enters through the suction, or low pressure port presented in light shade. It thus fills the spaces between the lobes, starting from the ends corresponding to A and C. As may be seen, the trapped volume in each chamber increases as rotation proceeds and the contact line between the rotors recedes. At the point where the maximum volume is filled, the inlet port terminates, and rotation proceeds without any further fluid admission in the region corresponding to the dark shaded area.

Viewed from Fig. 1b, it may be seen that the dark shaded area begins, from the end A and C, at the point where the main and gate rotor lobes start to re-engage. Thus, from that position, further rotation reduces the volume of gas trapped between the lobes and the housing. This causes the pressure to rise. At the position where the trapped volume is sufficiently reduced to achieve the required pressure rise, the ends of the rotors corresponding to D and B are exposed to an opening presented in light shade, which forms the high pressure or discharge port. Further rotation reduces the trapped volume causing the fluid to flow out through the high pressure port at approximately constant pressure. This continues until the trapped volume is reduced to virtually zero and all the gas between the lobes is expelled. The process is then repeated for each chamber.

The meshing action of the lobes, as they rotate, is the same as that of helical gears, but in addition, their shape must be such that at any contact position, a sealing line is formed between the rotors and between the rotors and the housing in order to prevent internal leakage between successive trapped passages. A further requirement is that the passages between the lobes should be as large as possible to maximize the fluid displacement per revolution. Also, the contact forces between the rotors should be low to minimize internal friction losses. A typical screw rotor profile is shown in Fig. 2 with the sealing lines, as well as the clearance distribution between two rotor racks in the transverse cross section are presented far above.

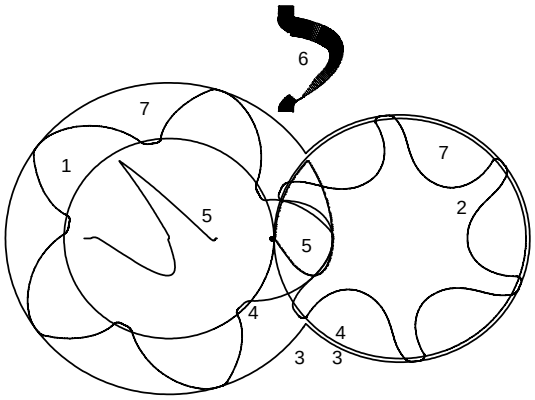

Fig. 2 Screw rotor profile
1: Main; 2: Gate; 3: Rotor external; 4: Pitch circles; 5: Sealing line; 6: Clearance distribution presented as distance between two rotor racks; 7: Rotor flow area between the rotors and housing

Screw machines have a number of advantages over other positive displacement types. Firstly, unlike reciprocating machines, the moving parts all rotate, and hence can run at much higher speeds. Secondly, unlike vane machines, the contact forces within them are low, which makes them very reliable. Thirdly, and far less well known, unlike the reciprocating, scroll, and vane machines, all the sealing lines of contact, which define the boundaries of each cell chamber, decrease in length as the size of the working chamber decreases and the pressure within it rises, and this minimizes the escape of gas from the chamber due to leakage during the compression or expansion process.

Serious efforts to develop screw machines began in the 1930s, when Lysholm (1942), a Swedish engineer, used a screw compressor as a part of the gas turbine, and all modern developments in this machine stem from his pioneering work. From then until the mid 1960s, the main drawback to their widespread use was the inability to manufacture rotors accurately at an acceptable cost. Two developments then accelerated their adoption. The first was the development of milling machines for thread cutting. The use of this for rotor manufacture enabled these components to be made far more accurately at an acceptable cost. The second occurred in 1973, when Svenska Rotor Maskiner (SRM), in Sweden, introduced the 'A' profile, which reduced the internal leakage path area, known as the blow hole by 90%. Screw compressors could then be built with efficiencies approximately equal to those of reciprocating machines, and the use of screw compressors, especially of the oil flooded type, was then proliferated.

To perform effectively, screw compressor rotors must meet the meshing requirements of gears while maintaining a seal along their length to minimize leakage at any position on the band of rotor contact. It follows that the compressor efficiency depends on both the rotor profile and the clearances between the rotors and between the rotors and the compressor housing.

The efficient operation of screw compressors is mainly dependent on a proper rotor design. An additional and important requirement or the successful design of all types of compressor is an ability to predict accurately the effects on performance of the change in any design parameter such as clearance, rotor profile shape, oil or fluid injection position and rate, rotor diameter, proportions, and speed.

Screw compressor rotors are usually manufactured on specialized machines by the use of formed milling or grinding tools. Machining accuracy achievable today is high, and tolerances in rotor manufacture are of the order of 5 μm around the rotor lobes. Holmes and Stephen (1999) reported that an even higher accuracy was achieved on the new Holroyd vitrifying thread-grinding machine, thus keeping the manufacturing tolerances within 3 μm even in a large batch production. This means that, as far as rotor production alone is concerned, clearances between the rotors can be as small as 12 μm.

Now, when tight clearances are introduced and internal compressor leakage rates become small, further improvements are only possible by the introduction of more refined design principles. The main requirement is to improve the rotor profiles so that the internal flow area through the compressor is maximised while the leakage path is minimized as well as the internal friction due to relative motion between the contacting rotor surfaces. As precise manufacture permits rotor clearances to be reduced, the likelihood of direct rotor contact is increased. Hard rotor contact leads to increase of temperature because of friction, and consequently deformation of the gate rotor, increased contact forces, and ultimately rotor seizure. Hence the profile should be designed so that the risk of seizure is minimized.

2 Review of contemporary rotor profiles of screw compressors

A practice predominantly used today for generation of screw compressor rotor profiles is to create primary profile curves on one of the real screw rotors and to generate a corresponding secondary profile curve on another rotor using some appropriate conditions of conjugate action. Any curve can be used as the primary one, but traditionally circle is the most commonly used.

Symmetric circular profile consists of circles only, Lysholm's asymmetric profile apart of circles which are located at the rotor pitch circle introduces a set of cycloids on the high pressure side forming the first asymmetric screw rotor profile. The SRM asymmetric profile employs an eccentric circle on the low pressure side of the gate rotor, followed by the

SKBK profile introducing the same on the main rotor. In both cases evolved curves were given analytically as epicycloids or hypocycloids. SRM 'D' profile consists exclusively of circles, and all of them were eccentrically positioned on the main or gate rotor.

All patents followed give primary curves on one rotor, and secondary, generated curves on another one, all probably based on derivations of the classical gearing or other similar conditions. More recently, the circles are gradually replaced by other curves, such as ellipses in Fusheng profiles, parabolae in Compair and Hitachi profiles, and hyperbolae in Hanbel hyper profiles. The hyperbola in the latest profile seems to be the most appropriate replacement giving the best ratio of the rotor displacement to seal line length.

Another practice to generate screw rotor profile curves is to use imaginary or nonphysical rotors. Since all gearing equations are independent of the coordinate system in which they are expressed, it is possible to define primary arcs as given curves using a coordinate system, which is independent of both rotors. By this means, in many cases, the defining equations may be simplified. Also, the use of one coordinate system to define all the curves further simplifies the design process. Typically, the template is specified in a rotor independent coordinate system. The same is valid for a rotor of infinite radius which is a rack.

From this, a secondary arc on some of the rotors is obtained by the procedure, which is called rack generation. The first ever published patent on rack generation lacks of practicality but conveniently uses the theory (Menssen, 1977). Later, a good basis for the screw compressor profile generation was given (Rinder, 1987; Stosic, 1996a; 1996b; 1996c; 1996d).

An efficient screw compressor needs a rotor profile, which has a large flow cross section area, a short sealing line, and a small blow-hole area. The larger the cross section area, the higher the flow rate for the same rotor sizes and rotor speeds. Shorter sealing lines and a smaller blow hole reduce leakages. Higher flow and smaller leakage rates both increase the compressor volumetric efficiency, which is the rate of flow delivered as a fraction of the sum of the flow plus leakages. This in turn increases the adiabatic efficiency, because less power is wasted in the compression of gas which is recirculated internally. The optimum choice between blow hole and flow areas depends on the compressor duty since for low pressure differences the leakage rate will be relatively small, and hence the gains achieved by a large cross section area may outweigh the losses associated with a larger blow hole. Similar considerations determine the best choice for the number of lobes, since fewer lobes imply greater flow area but increased pressure difference between them.

The search for new profiles has been both stimulated and facilitated by recent advances in mathematical modeling and computer simulation. These analytical methods may be combined to form a powerful tool for process analysis and optimization and thereby eliminate the earlier approach of intuitive changes, verified by tedious trial and error testing. As a result, this approach to the optimum design of screw rotor lobe profiles has substantially evolved over the past few years, and is likely to lead to further improvements in machine performance in the near future.

The majority of screw compressors are still manufactured with a configuration of 4/6 (four and six lobes in the main and gate rotors respectively, with both rotors of the same outer diameter). This configuration is a compromise, which has favorable features for both, dry and oil-flooded compressor applications, and is used for air and refrigeration or process gas compressors. However, other configurations, like 5/6 and 5/7, and recently 4/5 and 3/5, are becoming increasingly popular. Five lobes in the main rotor are suitable for higher compressor pressure ratios, especially if combined with larger helix angles. The 4/5 arrangement has emerged as the best combination for oil-flooded applications of moderate pressure ratios. The 3/5 is favored in dry applications, because it offers a high gear ratio between the gate and main rotors which may be taken advantage of to reduce the required drive shaft speed.

Fig. 3 shows pairs of screw compressor rotors plotted together for comparison. They are given by their commercial names or by names which denote their patent.

3 Design of screw compressor housings and choice of bearings

Although advanced rotor profiles are a necessary condition for a screw compressor to be efficient, all

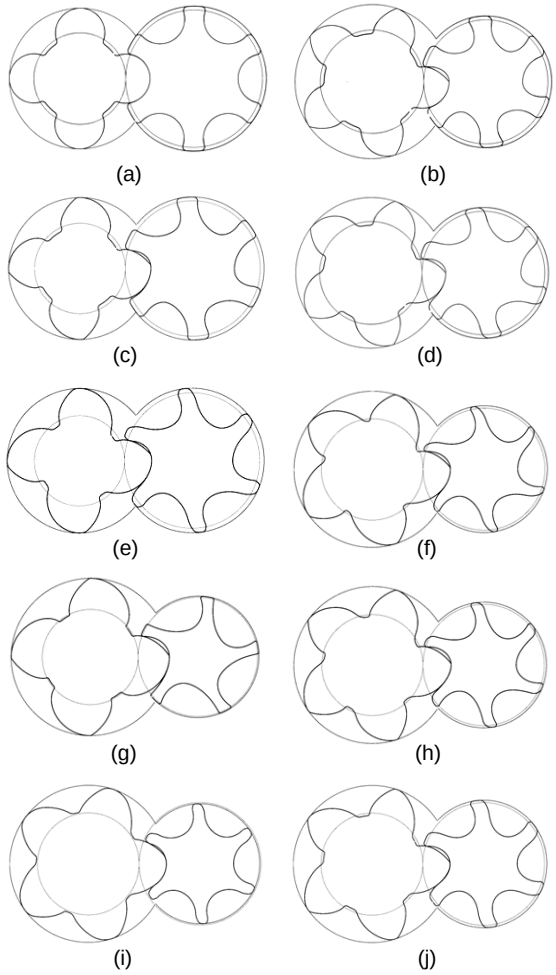

Fig. 3 Most popular screw compressor rotors today
(a) Symmetric circular profile (Robert, 1952); (b) Lysholm's asymmetric profile (Lysholm, 1967); (c) SRM 'A' profile (Shibbye, 1979); (d) SKBK profile (Amosov *et al.*, 1977); (e) SRM 'D' profile (Astberg, 1982); (f) Fusheng profile (Lee, 1988); (g) Compair profile (Hough *et al*., 1984); (h) Hyper profile (Chen, 1995); (i) Rinder's profile (Rinder, 1987); (j) 'N' profile (Stosic, 1996)

other components must be designed to take advantage of their potential if the full performance gains are to be achieved. Thus rotor to housing clearances, especially at the high pressure end must be properly selected.

A contact force between rotors, which is determined by the torque transferred between rotors, plays a key role in compressors of a direct rotor contact. The contact force is relatively small in the case of a main rotor driven compressor. In the case of a gate rotor drive, the contact force is substantially larger, and this case should be excluded from any serious consideration.

The same oil is used for oil flooding and for bearing lubrication, but the supply to and evacuation from the bearings are separate to minimize the friction losses. Oil is injected into the compressor chamber at the place where thermodynamic calculations show the gas and oil inlet temperature to coincide. The position is defined on the rotor helix with the injection hole located so that the oil enters tangentially in line with the gate rotor tip in order to recover as much as possible the oil kinetic energy.

To minimize the flow losses in the suction and discharge ports, the following features are included. The suction port is positioned in the housing to let the gas enter with the fewest possible bends, and the gas approach velocity is kept low by making the flow area as large as possible. The discharge port size is first determined by estimating the built-in-volume ratio required for optimum thermodynamic performance. It is then increased in order to reduce the exit gas velocity and hence obtain the minimum combination of internal and discharge flow losses. Therefore, since the housing should be carefully dimensioned to minimize its weight, the reinforcing bars across the suction port are placed to improve its rigidity at higher pressures. Screw compressor is a very simple heat machine with only a few moving parts, two rotors and usually four to six bearings. Screw compressor designs evolved through history to very typical forms. It must be added that recent advances in the development of advanced low friction rolling element bearings highly contribute to the result.

Any production imperfection in the bearing housing, like displacement or eccentricity, will change the rotor position and thereby influence the compressor behavior.

A tendency is to get as small as possible machine to produce and perform satisfactorily. This means that the rotor tip speed is kept as high as possible, but still in some limits to result in an acceptable machine efficiency. It is almost a rule to apply rolling bearings wherever possible to use their advantage of smaller clearances compared with dynamic journal bearings. The ports are made as wide as possible to minimize suction and discharge gas speeds. All these give very similar screw compressor designs, and departures from them are almost negligible.

Screw machines are used today for a variety of applications both as compressors and expanders. They operate on a variety of working fluids which may be gases, dry vapors, or multi-phase mixtures with phase changes taking place within the machine. Their mode of operation may be without internal lubrication, oil flooded or with other fluids injected during the compression or expansion process. For optimum performance from such machines, a specific design and operating mode is needed for each application. Hence, it is not possible to produce efficient machines by the specification of a universal rotor configuration or set of working parameters, even for a restricted class of compressors. Because of this variety of uses and the geometric complexity of these machines, detailed thermodynamic analysis and study of the influence of various design parameters on the machine performance are probably more important, though less straightforward, than for other types of machine which perform similar functions. It follows that a set of well defined criteria governed by an optimization procedure is a prerequisite for achieving an optimum performance for each application. Such guidelines are also essential for further improvement of existing screw compressor designs, and broadening the range of uses for these machines. More detailed information on screw compressor design can be found in Stosic *et al*. (2005).

An example of a screw compressor layout is given in Fig. 4.

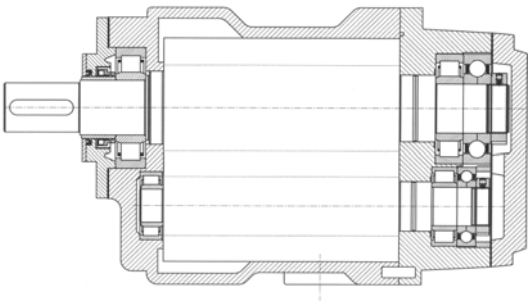

Fig. 4 Drawing of typical screw rotors and housing assembled in a screw compressor with low pressure side bearings on the left and high pressure side bearings right

4 Geometry of screw compressor rotors

The rotor lobe profiles have to be defined together with the remaining rotor parameters before the rotor and housing geometry can be fully specified. To explain the rotor profiling principles, a default profile version is used, so called 'demonstrator', which can take any realistic combination of numbers of lobes in the main and gate screw rotors. However, any other known or a completely new profile can be generated, with little modification. Such profiles must, of course, satisfy geometrical constraints in order to obtain a realistic solution. The subroutines to calculate a majority of the existing screw compressor rotor profiles can be obtained upon request.

4.1 Envelope method as a basis for profiling of screw compressor rotors

The envelope method is used here as a basis for generation of the screw compressor rotor profile. The method states that two surfaces are in mesh if each generates or envelops the other under a specified relative motion. This is becoming increasingly popular, and details of how it may be applied to screw compressor rotor profiles, have been given by Stosic (1998). Although a generation screw compressor rotors can be fully regarded as a 2D problem, a 3D approach is given here as a general starting point, which further gives an opportunity to generate the rotor tools from the same equations. The envelope method was used for screw compressor rotor generation on screw compressors (Andreev, 1961; Xing 2000). A similar approach was applied, and the envelope method was used as a basis for generation of screw compressor rotors and rotor manufacturing tools (Tang and Fleming, 1994).

Following Stosic (1998), screw compressor rotors are treated here as crossed helical gears with non-parallel and non-intersecting axes (Fig. 5). $x_{01}y_{01}$ and $x_{02}y_{02}$ are the point coordinates at the end rotor section in the coordinate systems fixed to the main and gate rotors. Σ is the rotation angle around x axis. Rotation of the rotor shaft around z axis is the natural rotor movement in its bearings. While the main rotor rotates through angle θ, the gate rotor rotates through angle $\tau=(r_{1w}/r_{2w})\theta=(n_2/n_1)\theta$, where r_w and n are the pitch circle radii and number of rotor lobes, respectively; the subscripts '1' and '2' relate to the main and gate rotors, respectively, while 'w' refers to the pitch circle.

The procedure starts with a given, or generating surface $\boldsymbol{r}_1(t,\theta)$ for which a meshing, or generated surface is to be determined:

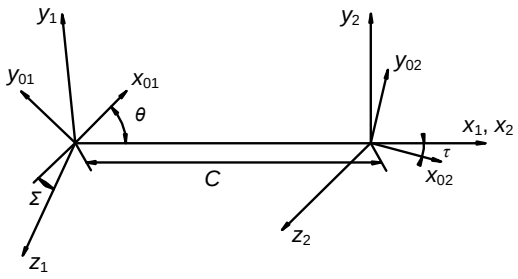

Fig. 5 Coordinate system of helical gears with non-parallel and non-intersecting axes

$$\begin{aligned}\boldsymbol{r}_1 &= \boldsymbol{r}_1(t,\theta)=\left[x_1, y_1, z_1\right]\\ &=\left[x_{01}\cos\theta - y_{01}\sin\theta, x_{01}\sin\theta + y_{01}\cos\theta, p_1\theta\right],\end{aligned} \tag{1}$$

$$\begin{aligned}\frac{\partial \boldsymbol{r}_1}{\partial t} &= \left[\frac{\partial x_1}{\partial t}, \frac{\partial y_1}{\partial t}, 0\right]\\ &=\left[\frac{\partial x_{01}}{\partial t}\cos\theta - \frac{\partial y_{01}}{\partial t}\sin\theta, \frac{\partial x_{01}}{\partial t}\sin\theta + \frac{\partial y_{01}}{\partial t}\cos\theta, 0\right],\end{aligned} \tag{2}$$

$$\frac{\partial \boldsymbol{r}_1}{\partial \theta} = \left[\frac{\partial x_1}{\partial \theta}, \frac{\partial y_1}{\partial \theta}, p_1\right] = \left[-y_{01}, x_{01}, p_1\right], \tag{3}$$

where p is a rotor lead given for the unit rotor rotation angle, and t is the rotor parameter. A family of such generated surfaces is given in parametric form by $\boldsymbol{r}_2(t, \theta, \tau)$, where t is a profile parameter while θ and τ are motion parameters:

$$\begin{aligned}\boldsymbol{r}_2 &= \boldsymbol{r}_2(t,\theta,\tau)=\left[x_2, y_2, z_2\right]\\ &=\left[x_1 - C, y_1\cos\Sigma - z_1\sin\Sigma, y_1\sin\Sigma + z_1\cos\Sigma\right]\\ &=\left[x_{02}\cos\tau - y_{02}\sin\tau, x_{02}\sin\tau + y_{02}\cos\tau, p_2\tau\right],\end{aligned} \tag{4}$$

$$\begin{aligned}\frac{\partial \boldsymbol{r}_2}{\partial \tau} &= \left[-y_2, x_2, p_2\right]\\ &=\left[x_{02}\sin\tau + y_{02}\cos\tau, x_{02}\cos\tau - y_{02}\sin\tau, p_2\right]\\ &=\left[p_1\theta\sin\Sigma - y_1\cos\Sigma, p_2\sin\Sigma + (x_1 - C)\cos\Sigma,\right.\\ &\quad \left. p_2\cos\Sigma - (x_1 - C)\sin\Sigma\right],\end{aligned} \tag{5}$$

where C is the rotor centre distance.

The envelope equation, which determines meshing between the surfaces $\boldsymbol{r}_1$ and $\boldsymbol{r}_2$ is defined as

$$\left(\frac{\partial \boldsymbol{r}_2}{\partial t}\times\frac{\partial \boldsymbol{r}_2}{\partial \theta}\right)\cdot\frac{\partial \boldsymbol{r}_2}{\partial \tau} = 0. \tag{6}$$

Together with equations for these surfaces, it completes a system of equations. If a generating surface 1 is defined by the parameter t, the envelope may be used to calculate another parameter θ, now a function of t, as a meshing condition to define a generated surface 2, now the function of both t and θ. The cross product in the envelope equation represents a normal surface, and $\frac{\partial \boldsymbol{r}_2}{\partial \tau}$ is a relative sliding velocity of two single points on the surfaces 1 and 2, which together form the common tangential point of contact of these two surfaces. Since the equality to zero of a scalar triple product is an invariant property under the applied coordinate system and since the relative velocity may be concurrently represented in both coordinate systems, a convenient form of the meshing condition is defined as

$$\left(\frac{\partial \boldsymbol{r}_1}{\partial t}\times\frac{\partial \boldsymbol{r}_1}{\partial \theta}\right)\cdot\frac{\partial \boldsymbol{r}_1}{\partial \tau} = -\left(\frac{\partial \boldsymbol{r}_1}{\partial t}\times\frac{\partial \boldsymbol{r}_1}{\partial \theta}\right)\cdot\frac{\partial \boldsymbol{r}_2}{\partial \tau} = 0. \tag{7}$$

Insertion of previous expressions into this envelope condition leads to

$$\begin{aligned}&\left[C - x_1 + (p_1 - p_2)\cot\Sigma\right]\left(x_1\frac{\partial x_1}{\partial t} + y_1\frac{\partial y_1}{\partial t}\right)\\ &+ p_1\left[p_1\theta\frac{\partial y_1}{\partial t} + (p_2 - C\cot\Sigma)\frac{\partial x_1}{\partial t}\right] = 0.\end{aligned} \tag{8}$$

This equation is applied here to derive the condition of meshing action for crossed helical gears of uniform lead with nonparallel and nonintersecting axes. The method constitutes a gear generation procedure which is generally applicable. It can be used for synthesis purposes of screw compressor rotors, which are effectively helical gears with parallel axes. Formed tools for rotor manufacturing are crossed helical gears on non-parallel and non-intersecting axes with a uniform lead, as in the case of hobbing, or with no lead as in formed milling and grinding. Templates for rotor inspection are the same as planar rotor hobs. In all these cases the tool axes do not intersect the rotor axes.

Accordingly the notes present an application of the envelope method to produce a meshing condition for crossed helical gears. The screw rotor gearing is

then given as an elementary example of its use while a procedure for generation of a hobbing tool is given as a complex case.

The shaft angle Σ, centre distance C, and unit leads of two crossed helical gears p_1 and p_2 are not interdependent. A meshing of crossed helical gears is still preserved: both gear racks have the same normal cross section profile, and the rack helix angles are related to the shaft angle as $\Sigma=\psi_{rw1}+\psi_{rw2}$. This is achieved by the implicit shift of the gear racks in the x direction forcing them to adjust accordingly to the appropriate rack helix angles. This certainly includes special cases, like that of gears which may be orientated so that the shaft angle is equal to the sum of gear helix angles: $\Sigma=\psi_1+\psi_2$. Furthermore, a centre distance may be equal to the sum of the gear pitch radii: $C=r_{1w}+r_{2w}$.

Pairs of crossed helical gears may be with either both helix angles of the same sign or each of opposite sign, left or right handed, depending on the combination of their lead and shaft angle Σ.

Eq. (8) can be solved only by numerical methods. For the given parameter t, the coordinates x_{01} and y_{01}, and their derivatives $\frac{\partial x_{01}}{\partial t}$ and $\frac{\partial y_{01}}{\partial t}$ are known. A guessed value of parameter θ is then used to calculate x_1, y_1, $\frac{\partial x_1}{\partial t}$, and $\frac{\partial y_1}{\partial t}$. A revised value of θ is then derived, and the procedure repeated until the difference between two consecutive values becomes sufficiently small.

For given transverse coordinates and derivatives of gear 1 profile, θ can be used to calculate the x_1, y_1, and z_1 coordinates of its helicoids surface. The gear 2 helicoids surface may then be calculated. Coordinate z_2 can then be used to calculate τ, and finally, its transverse profile point coordinates x_2 and y_2 can be obtained.

A number of cases can be identified from this analysis:

1. When $\Sigma=0$, the equation meets the meshing condition of screw machine rotors and also helical gears with parallel axes. For such a case, the gear helix angles have the same value, but the opposite sign and the gear ratio $i=p_2/p_1$ are negative. The same equation may also be applied for the generation of a rack formed from gears. Additionally, it describes the formed planar hob, front milling tool, and the template control instrument.

2. If a disc formed milling or grinding tool is considered, it is sufficient to place $p_2=0$. This is a singular case when tool free rotation does not affect the meshing process. Therefore, a reverse transformation cannot be obtained directly.

3. The full scope of the meshing condition is required for the generation of the profile of a formed hobbing tool. Therefore, the most complicated type of gear can be generated from Eq. (8).

4.2 Direct digital simulation

A standard intrinsic feature of perhaps every existing design software package is to extract the overlapping areas of planar shapes or volumes of spatial bodies. It can be conveniently used to find a corresponding profile from a given profile. This subtraction may either be static, when the overlapping elements are extracted from the stationary assembly, or dynamic, when the subtraction is performed for a sequence of succeeding positions to give a generated profile or body over a complete cycle. All kind of relative motions can be imposed between the elements, and thus a variety of gear pairs can be designed on parallel, intersecting or nonintersecting and nonparallel axes. A known profile will therefore cut the required shape from a blank with an arbitrary starting shape. This feature enables non-specialists to generate their own rotor profiles without knowledge of comprehensive mathematical methods or use of specialized generation software tools. More details on direct digital simulation of screw compressor rotors can be found in Stosic *et al.* (2008). Application of direct digital simulation in generation of a gate rotor from its main counterpart is presented in Fig. 6.

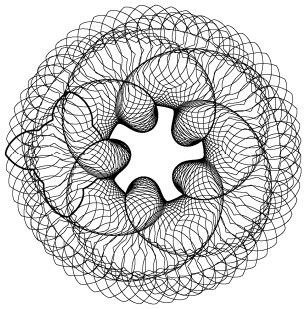

Fig. 6 Example of a gate rotor enveloped by its main counterpart using direct digital simulation

4.3 Meshing of rotor profiles

Screw machine rotors have parallel axes and a uniform lead, and they are therefore a form of helical gears (Fig. 7). Centre distance for this particular case is $C=r_{1w}+r_{2w}$. Rotors make lines contact, and the meshing criterion in the transverse plane perpendicular to their axes is the same as that of spur gears. Although spur gear meshing fully defines helical screw rotors, it may be more convenient to use the envelope condition for crossed helical gears and simplify it by setting $\Sigma=0$, to get the required meshing condition.

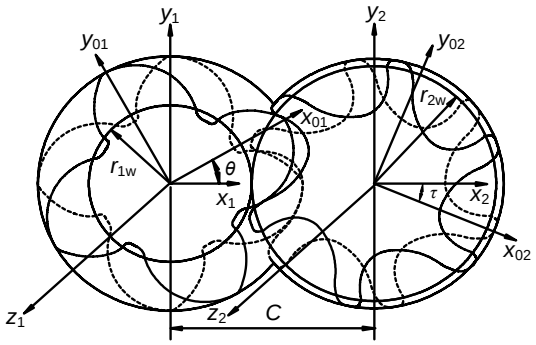

Fig. 7 Screw compressor rotors with parallel shafts and their coordinate systems

To start the procedure of rotor profiling, the profile point coordinates in the transverse plane of one rotor, x_{01} and y_{01} and their first derivatives, either $\frac{\partial x_{01}}{\partial t}$ and $\frac{\partial y_{01}}{\partial t}$ or $\frac{\mathrm{d}y_{01}}{\mathrm{d}x_{01}}$ must be known. This profile may be specified on either the main or gate rotors or in sequence on both. The primary profile may also be defined as a rack.

Since $\Sigma=0$, the general meshing condition presented in Eq. (8) reduces for a screw machine rotor to

$$\frac{\mathrm{d}y_{01}}{\mathrm{d}x_{01}}\left(ky_{01}-\frac{C}{i}\sin\theta\right)+kx_{01}+\frac{C}{i}\cos\theta=0, \quad (9)$$

where $i=p_2/p_1$ and $k=1-1/i$. Eq. (9) can be solved only numerically, similarly as its original. θ still can be obtained only numerically. Once obtained, the distribution of θ along the profile may be used to calculate the meshing rotor profile point coordinate, as well as to determine the sealing lines and paths of proximity between the two rotors. Rotor rack coordinates may also be calculated from the same θ distribution.

Since $\tau=\theta/i$ for parallel axes, the meshing profile equations of the gate rotor in the transverse plane are calculated as

$$\begin{cases} x_{02}=x_{01}\cos k\theta-y_{01}\sin k\theta-C\cos\dfrac{\theta}{i}, \\ y_{02}=x_{01}\sin k\theta+y_{01}\cos k\theta+C\sin\dfrac{\theta}{i}. \end{cases} \quad (10)$$

Rack coordinates can be obtained uniquely if the rack-to-rotor gear ratio i tends to infinity:

$$\begin{cases} x_{0\mathrm{r}}=x_{01}\cos\theta-y_{01}\sin\theta, \\ y_{0\mathrm{r}}=x_{01}\sin\theta+y_{01}\cos\theta-r_1\theta. \end{cases} \quad (11)$$

Conversely, if the gate rotor curves are given, generated curves will be placed on the gate rotor, and similar equations with substituted indices will be used to generate the main rotor profile.

However, if the primary curves are given on the rack, their coordinates $x_{0\mathrm{r}}$ and $y_{0\mathrm{r}}$, as well as their first derivatives, $\frac{\partial x_{0\mathrm{r}}}{\partial t}$ and $\frac{\partial y_{0\mathrm{r}}}{\partial t}$, or $\frac{\mathrm{d}y_{0\mathrm{r}}}{\mathrm{d}x_{0\mathrm{r}}}$ should be known, and the generated curves will be calculated at the rotors as

$$\begin{cases} x_{01}=x_{0\mathrm{r}}\cos\theta-(y_{0\mathrm{r}}-r_{1\mathrm{w}})\sin\theta, \\ y_{01}=x_{0\mathrm{r}}\sin\theta+(y_{0\mathrm{r}}-r_{1\mathrm{w}})\cos\theta, \end{cases} \quad (12)$$

after the meshing condition is obtained from

$$\frac{\mathrm{d}y_{0\mathrm{r}}}{\mathrm{d}x_{0\mathrm{r}}}(r_{1\mathrm{w}}\theta-y_{0\mathrm{r}})-(r_{1\mathrm{w}}-x_{0\mathrm{r}})=0. \quad (13)$$

The rack meshing condition θ can be solved directly and does not require a numerical procedure in its evaluation, which is another advantage of the rack generation method.

The presented procedure to solve the meshing condition numerically or directly enables introduction of a variety of primary arc curves and basically offers a general procedure. Further on, a numerical derivation of primary arcs enables a totally general approach when only the coordinates of the primary curves must be known, not their derivatives. In such a case, any

analytical functions and even discrete point functions can be used as primary arcs. This approach introduces an additional simplicity into the procedure. Only the primary arcs should be given, secondary ones are not derived, and they are evaluated automatically by means of the numerical procedure.

The sealing line of screw compressor rotors is somewhat similar to the gear contact line. Since there exists a clearance gap between rotors, the sealing line is a line consisting of points of the most proximate rotor position. Its coordinates are x_1, y_1, and z_1, and they are calculated for the same θ distribution. The most convenient practice to obtain an interlobe clearance gap is to consider the gap as the shortest distance between two rotor racks of the main and gate rotor sealing points in the cross section normal to the rotor helicoids.

The rotor racks, obtained from the rotors by the reverse procedure, can include all manufacturing and positioning imperfections. Therefore, the resulting clearance distribution may represent real life compressor clearances. From normal clearances, a transverse clearance gap may be obtained by the appropriate transformation.

As it has already been mentioned in this section, the profile point coordinates in the transverse plane of one rotor, x_{01} and y_{01}, and their first derivatives, either $\frac{\partial x_{01}}{\partial t}$ and $\frac{\partial y_{01}}{\partial t}$ or $\frac{\mathrm{d}y_{01}}{\mathrm{d}x_{01}}$ must be known. Since the rotor coordinates are integrals of their derivatives, it appears that only derivatives must be known to be able to generate the whole rotor profile from their initial condition. More information on this method is given in Stosic (2005).

For a further analysis of the compressor geometry, several generic definitions are introduced here. A centre distance between the rotors axes is $C=r_{1w}+r_{2w}$, where r_{1w} and r_{2w} are radii of the main and gate rotor pitch circles, respectively. A rotor gear ratio is $i=r_{2w}/r_{1w}=n_2/n_1$, where n_1 and n_2 are now numbers of lobes on the main and gate rotors. Since the screw compressor rotors are of 3D bodies, a helix angle ψ is defined at a rotor radius, while ψ_w corresponds to the pitch circle, $\tan\psi/\tan\psi_w=r/r_w$. Helix angle defines a rotor lead h, which can be given relative to the unit angle by $p=h/2\pi$. Rotor length L, wrap angle φ, and lead are interrelated with $L/\varphi=h/2\pi=p$. If the rotors are unwrapped, a simple relation between the wrap and helix angles can be established, $\tan\psi_w=\varphi r_w/h=2\pi r_w/L$.

Rotor displacement is a product of the rotor length and its cross section area, which is denoted number 7 as presented in Fig. 2.

4.4 Features of 'N' rotor profiles

Following is a detailed presentation of rotor creation by the rotor generation and rack generation procedures. The rotor profile in the first case is a hypothetic one, and it has not yet been used in practice and no compressors have ever been manufactured around it. However, this profile has been frequently used for the purpose of education, and the same rotor profile is given as a demonstrator in Demo software. Furthermore, this profile may very conveniently be used as a basis for individual development of screw compressor rotors, and such use is encouraged here. The second example is 'N' rotor generated from its rack and this profile is protected by international patents (Stosic, 1996a; 1996b; 1996c; 1996d).

4.4.1 Demonstrator rotor profile ('N' rotor generated)

Demonstrator profile is a rotor generated 'N' profile and it is not a patented rack generated 'N' profile. A primary or generating lobe profile of the demonstrator consists of circles only, it is given on the main rotor, and the profile is divided into several segments (Fig. 8a). The lobe segments of this profile are essentially parts of circles on one of the rotor and trochoid curves corresponding to the circles on the opposite rotor.

The following summarizes the specific expressions for the *xy* coordinates of the lobe profiles for the main screw rotor, with respect to the centre of the rotor O_1. Given are the pitch radii, r_{1w} and r_{1w}, and rotor radii r, r_0, r_2, r_3, and r_4. External and internal radii are calculated as $r_{1e}=r_{1w}+r$ and $r_{1i}=r_{1w}-r_0$ for the main and gate rotors, respectively (Fig. 8b).

When all segments of the main rotor are known, they are used as source curves. The gate rotor lobe in whole is now generated by the meshing procedure described in the previous section.

Although being plainly simple, almost generic, the demonstrator profile contains all features which characterize modern screw rotor profiles. Pressure angles on the both, flat and round profile lobes are different of zero, which is a prerequisite for a

successful manufacturing. The profile is generated by the curves and not by points, which enhance its manufacturability even more. By changing its parameters, r_1, r_2, r_3, and r_4 (Fig. 8), a variety of profiles can be generated, some of them with positive gate rotor torque, some of them suitable for low pressure ratios, and some of them for high pressure ratio compression. The profile is fully computerized and can be used for demonstration, teaching, and development purposes.

4.4.2 City 'N' rack generated rotor profile

Patented 'N' rotors are calculated by the rack generation procedure. This distinguishes 'N' rotors from almost any other screw compressor rotors existing today in the screw compressor community. A large blow-hole area, characterizing the rack generated rotors, is in 'N' rotors overcome by generating the high pressure side of a rack by means of a rotor conjugate action which undercuts a single appropriate curve on the rack. Such rack is then used for profiling both the main and gate rotors. The method and its extensions were used to create a number of different rotor profiles (Stosic and Hanjalic, 1997).

The following is a brief description of a rack generated 'N' rotor profile, typical for a family of rotor profiles designed for the efficient compression of air, common refrigerants, and a number of process gases. Rotors are generated by the combined rack-rotor generation procedure. Its features are such that it may be readily modified further to optimize performance for any specific application. The coordinates of all primary arcs on the rack are summarized here relative to the rack coordinate system. The lobe of the rack is divided into several arcs (Fig. 9a).

All curves at 'N' profile are given as a general arc form, from which circles, parabolae, ellipses, and hyperbolae are all easily generated.

Segment *DE* is a straight line on the rack, *EF* is a circular arc of radius r_4, *FG* is a straight line for the

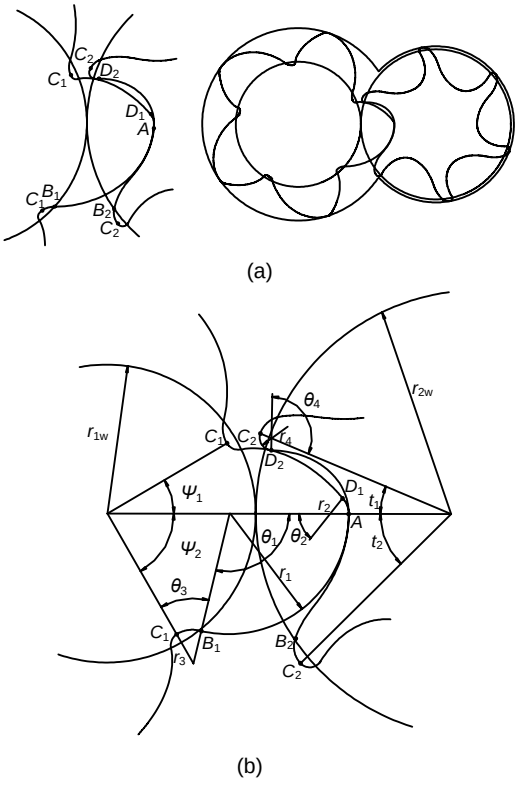

Fig. 8 Demonstrator 'N' profile (a) with its details (b)
Capital letters denote the divisions between the profile segments, and each segment is defined separately by its characteristic angles

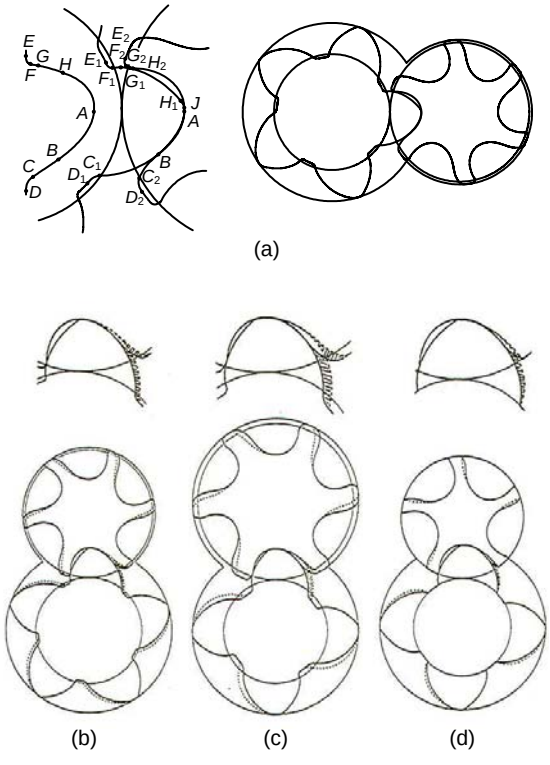

Fig. 9 'N' rotors (a) compared with 'Sigma' (b), SRM 'D' (c), and 'Cyclon' (d) rotors
Capital letters denote the divisions between the profile arcs, and each arc is defined separately

upper involute, while *GH* on the rack is a meshing curve generated by the circular arc G_2H_2 on the gate rotor. Segment *HJ* on the rack is a meshing curve generated by the circular arc H_1J_1 of the radius r_2 on the main rotor. Segment *JA* is a circular arc of radius *r* on the rack, *AB* is an arc which can be either circle, or prabola or hyperbola or ellipse, *BC* is a straight line on the rack matching the involute on the rotor round lobe, and *CD* is a circular arc on the rack, radius r_3.

Although the full evaluation of a rotor profile requires more than just a geometric assessment, some of the key features of the 'N' profile may be readily appreciated by comparing it with three most popular screw rotor profiles: 'Sigma' (Bammert, 1979), SRM 'D' (Astberg, 1982), and 'Cyclon' (Hough and Morris, 1984) profiles (Fig. 9). As shown in Fig. 9, 'N' profiles have a greater throughput and a stiffer gate rotor for all cases, while other characteristics such as blow-hole area, confined volume, and high pressure sealing line lengths are identical in the designs compared. Also, the low pressure sealing lines are shorter, but this is less important because the corresponding clearance can be kept small. The blow-hole area may be controlled by adjustment of the tip radii on both the main and gate rotors and also by making the gate outer diameter equal to or less than the pitch diameter. Also sealing lines can be kept very short by constructing most of the rotor profile from circles whose centres are close to the pitch circle. But, any decrease in the blow-hole area will increase the length of the sealing line on the flat rotor side. A compromise between these trends is therefore required to obtain the best result.

4.5 Rotor position in compressor bearings

A screw compressor, especially of the oil-flooded type, which operates with high pressure differences, is heavily loaded by axial and radial forces which are transferred to the housing by the bearings. Rolling element bearings are normally chosen for small and medium screw compressors and these must be carefully selected to obtain a satisfactory design. Usually, two bearings are employed on the discharge end of each of the rotor shafts in order to absorb the radial and axial loads separately. Also, the distance between the rotor centre lines is in part determined by the bearing size and internal clearance. Any production imperfection in the bearing housing, like displacement or eccentricity, will change the rotor position and thereby influence the compressor behavior.

The bearings, labeled 1 to 4 are presented in Fig. 10, as well as their clearances and manufacturing tolerances of the bearing bores, δ_x and δ_y in the *x* and *y* directions respectively. The rotor centre distance is *C*, and the axial span between the bearings is *a*.

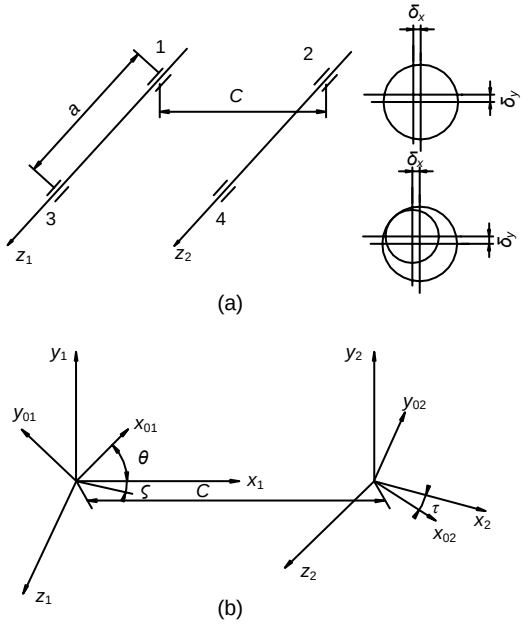

Fig. 10 Rotor shafts in the compressor housing and displacement in bearings (a) and coordinate systems of rotors with intersecting shafts (b)

All imperfections in the manufacture of screw compressor rotors should fall within and be accounted for by production tolerances. These are the wrong positions of the bearing bores, eccentricity of the rotor shafts, bearing clearances and imperfections, and rotor misalignment. Together, they account for the rotor shafts not being parallel. Let rotor movement δ_y in the *y* direction contain all displacements, and cause virtual rotation of the rotors around the x_1, and x_2 axes (Fig. 10). The movement δ_x can cause the rotor shafts to intersect. However, the movement δ_y causes the shafts to become non-parallel and non-intersecting. These both change the nature of the rotor position so that the shafts can no longer be regarded as parallel. The following analytical approach enables the rotor movement to be calculated and accounts for these changes.

Vectors $\boldsymbol{r}_1=[x_1,y_1,z_1]$ and $\boldsymbol{r}_2$, now represent the helicoid surfaces of the main and gate rotors on intersecting shafts:

$$\begin{aligned}\boldsymbol{r}_2&=\left[x_2,y_2,z_2\right]\\&=\left[x_1\cos\varsigma-z_1\sin\varsigma-C,y_1,x_1\sin\varsigma+z_1\cos\varsigma\right],\end{aligned}\tag{14}$$

$$\tan\varsigma=\delta_x/a,\tag{15}$$

where ς is the rotation about the y axis. Since this rotation angle is usually very small, Eq. (14) can be rewritten in a simplified form as $\boldsymbol{r}_2=[x_2,y_2,z_2]=[x_1-z_1\varsigma-C,\ y_1,x_1\varsigma+z_1]$.

The rotation ς will result in a displacement of $-z_1\varsigma$ in the x direction and a displacement of $x_1\varsigma$ in the z direction, while there is no displacement in the y direction. The displacement vector becomes $\Delta\boldsymbol{r}_2=[-z_1\varsigma,0,x_1\varsigma]$.

In the majority of practical cases, x_1 is small compared with z_1, and only displacement in the x direction needs to be considered. This means that rotation around the y axis will practically change the rotor centre distance only. Displacement in the z direction may be significant for the dynamic behavior of the rotors. Displacement in the z direction will be adjusted by the rotor relative rotation around the z axis, which can be accompanied by a significant angular acceleration. This may cause the rotors to lose contact at certain stages of the compressor cycle and thus create rattling, which may increase the compressor noise.

Since the rotation angle ς caused by displacement within the tolerance limits is very small, a 2D presentation in the rotor end plane can be applied, as is done in the next section.

As shown in Fig. 5 where the rotors on the non-parallel and non-intersecting axes are presented, vectors $\boldsymbol{r}_1=[x_1, y_1, z_1]$ and $\boldsymbol{r}_2$, given by Eqs. (1) and (4), now represent the helicoid surfaces of the main and gate rotors on the intersecting shafts:

$$\begin{aligned}\boldsymbol{r}_2&=\left[x_2,y_2,z_2\right]\\&=\left[x_1-C,y_1\cos\Sigma-z_1\sin\Sigma,y_1\sin\Sigma+z_1\cos\Sigma\right],\end{aligned}\tag{16}$$

$$\tan\Sigma=\delta_y/a.\tag{17}$$

Since angle Σ in Eq. (17) is very small, Eq. (16) can be rewritten in a simplified form as $\boldsymbol{r}_2=[x_2,y_2,z_2]=[x_1-C,y_1-z_1\Sigma,y_1\Sigma+z_1]$.

The rotation Σ will result in a displacement of $-z_1\Sigma$ in the y direction and a displacement of $y_1\Sigma$ in the z direction, while there is no displacement in the x direction. The displacement vector can be written as $\Delta\boldsymbol{r}_2=[0,-z_1\Sigma,y_1\Sigma]$.

Although, in the majority of practical cases, displacement in z direction is very small and therefore unimportant for consideration of rotor interference, it may play a role in the dynamic behavior of the rotors. The displacement in the z direction will be fully compensated by a regular rotation of the rotors around the z axis. However, the angular acceleration involved in this process may cause rotors to lose contact at some stages of the compressor cycle.

Rotation about the x axis is effectively the same as if the main or gate rotor rotated relatively through angle $\theta=-z_1\Sigma/r_{1\mathrm{w}}$ or $\tau=z_1\Sigma/r_{2\mathrm{w}}$ respectively, and the rotor backlash will be reduced by $z_1\Sigma$. Such an approach substantially simplifies the analysis and allows the problem to be presented in two dimensions in the rotor end plane.

Although the rotor movement described here are entirely 3D, their 2D presentation in the rotor end plane section can be used for analysis. The end plane clearance gap can then be obtained from the normal clearance by appropriate transformation.

If δ is the normal clearance between the rotor helicoid surfaces, the cross product of the $\boldsymbol{r}$ derivatives, $\left(\dfrac{\partial\boldsymbol{r}_1}{\partial t}\times\dfrac{\partial\boldsymbol{r}_1}{\partial\theta}\right)\cdot\dfrac{\partial\boldsymbol{r}_1}{\partial\tau}$, which defines the direction normal to the helicoids, can be used to calculate the coordinates of the rotor helicoids x_n and y_n from x and y to which the clearance was added as

$$\begin{cases}x_n=x+p\dfrac{\delta}{D}\dfrac{\mathrm{d}y}{\mathrm{d}t},\ y_n=y-p\dfrac{\delta}{D}\dfrac{\mathrm{d}x}{\mathrm{d}t},\\ z_n=\dfrac{\delta}{D}\left(x\dfrac{\mathrm{d}x}{\mathrm{d}t}+y\dfrac{\mathrm{d}y}{\mathrm{d}t}\right),\end{cases}\tag{18}$$

where the denominator D is given as

$$D=\sqrt{p^2\left(\frac{\mathrm{d}x}{\mathrm{d}t}\right)^2+p^2\left(\frac{\mathrm{d}y}{\mathrm{d}t}\right)+\left(x\frac{\mathrm{d}x}{\mathrm{d}t}+y\frac{\mathrm{d}y}{\mathrm{d}t}\right)^2}.\tag{19}$$

x_n and y_n serve to calculate new rotor end plane coordinates, x_{0n} and y_{0n}, with clearances from Eq. (18) for angles $\theta=z_n/p$ and τ respectively. x_{0n} and y_{0n} now

serve to calculate the transverse clearance δ_0 as the difference between them, as well as the original rotor coordinates x_0 and y_0.

If by any means, the rotors change their relative position, the clearance distribution at one end of the rotors may be reduced to zero at the flat side of the rotor lobes. In such a case, rotor contact will be prohibitively long on the flat side of the profile, where the dominant relative rotor motion is sliding. This indicates that rotor seizure will almost certainly occur in that region if the rotors come into contact with each other.

This situation indicates that a non-uniform clearance distribution should be applied to avoid hard rotor contact in rotor areas where sliding motion between the rotors is dominant.

4.6 Optimization of rotor profiles

The full rotor and compressor geometry, like the rotor throughput cross section, rotor displacement, sealing lines, and leakage flow cross section, as well as the suction and discharge port coordinates can be calculated from the rotor transverse plane coordinates and the rotor length and lead. The compressor built-in volume ratio is also used as an optimization variable. These values are later used as input parameters for the calculation of the screw compressor thermodynamic process, usually by use of mathematical models. The compressor geometry is recalculated for any variation of the input parameters. Computation of the instantaneous cross-sectional area and working volume can thereby be calculated repetitively in terms of the rotation angle.

Minimization of the output from the process equations leads to the optimum screw compressor geometry and operating conditions. These can be defined as either the highest flow and compressor volumetric and adiabatic efficiencies, or the lowest compressor specific power. More information on screw compressor optimization is given by Stosic *et al*. (2003), where an example is given involving nine variables. These include the rotor radii, defined by four rotor profile parameters, the built-in volume ratio, the compressor speed, and the oil flow, temperature, and injection position. A box constrained simplex method, which is a robust procedure that has already been applied in many other engineering applications, was used to find the local minima. It stochastically selects a simplex, which is a matrix of independent variables, and calculates the optimization target. In the case of the given examples, this was the minimum compressor specific power.

All effects are present and often they exert an opposing influence. The geometry of screw machines is dependent on a number of parameters whose best values to meet specified criteria can, in principle, be determined by a general multivariable optimization procedure. In practice, it is preferable to restrict the number of parameters to a few, which are known to be the most significant, and restrict the optimization to them only.

As any other optimization, the screw compressor profile and compressor design optimization must be considered with the extreme caution. Namely, since the multivariable optimization usually finds only the local minima, these may not necessarily be globally the best optimization result. Therefore, an extended calculation should inevitably be followed before a final decision on the compressor design is made.

5 Geometry of rotor manufacturing tools

This section describes generation of formed tools for screw compressor hobbing, milling, and grinding based on envelope gearing procedure. The hobbing tool as well as milling and grinding tools are presented in Fig. 11.

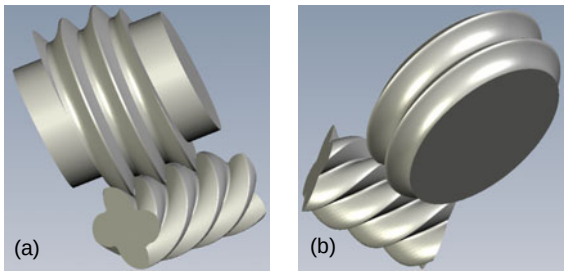

Fig. 11 Rotor manufacturing tools
(a) Hobbing tool; (b) Milling or grinding tool

5.1 Hobbing tools

A screw compressor rotor and its formed hobbing tool are meshing crossed helical gears with non-parallel and non-intersecting axes. The hob is simply a helical gear in which each tooth is referred to

as a thread. Owing to their axes not being parallel, there is only point contact between them whereas there is line contact between the screw machine rotors. The need to satisfy the meshing equation (Eq. (8)), leads to the rotor-hob meshing requirement for the given rotor transverse coordinate points x_{01} and y_{01} with their first derivative $\frac{\mathrm{d}y_{01}}{\mathrm{d}x_{01}}$. The hob transverse coordinate points x_{02} and y_{02} can then be calculated. These are sufficient to obtain the coordinate $R_2=\sqrt{{x_{01}}^2+{y_{01}}^2}$. The axial coordinate z_2, calculated directly, and R_2 are hob axial plane coordinates, which define the hob geometry.

Reverse calculation of the hob-screw rotor transformation, permits the determination of the transverse rotor profile coordinates which will be obtained as a result of the manufacturing process. These may be compared with those originally specified to determine the effect of manufacturing errors such as imperfect tool setting or tool and rotor deformation upon the final rotor profile.

For the purpose of reverse transformation, the hob longitudinal plane coordinates R_2 and z_2, and $\frac{\mathrm{d}R_2}{\mathrm{d}z_2}$ should be given. The axial coordinate z_2 is used to calculate $\tau=z_2/p_2$, which is then used to calculate the hob transverse coordinates:

$$x_{02}=R_2\cos\tau,\quad y_{02}=R_2\sin\tau. \tag{20}$$

These are then used as given coordinates to produce a meshing criterion and the transverse plane coordinates of the manufactured rotors by Eq. (8).

5.2 Milling and grinding tools

Formed milling and grinding tools may also be generated by placing p_2=0 into the general meshing Eq. (8) and then following the procedure of this section. The resulting meshing condition now is

$$\begin{aligned}&(C-x_1+p_1\cot\Sigma)\left(x_1\frac{\partial x_1}{\partial t}+y_1\frac{\partial y_1}{\partial t}\right)\\&+p_1\left(p_1\theta\frac{\partial y_1}{\partial t}-C\cot\Sigma\frac{\partial x_1}{\partial t}\right)=0.\end{aligned} \tag{21}$$

However, in this case, if one expects to obtain screw rotor coordinates from the tool coordinates, the singularity imposed does not permit the calculation of the tool transverse plane coordinates. The main meshing condition cannot therefore be applied. For this purpose another condition is derived for the reverse milling tool to rotor transformation, from which a meshing angle τ is calculated:

$$\begin{aligned}&\left(R_2+z_2\frac{\mathrm{d}z_2}{\mathrm{d}R_2}\right)\cos\tau+(p_1+C\cot\Sigma)\frac{\mathrm{d}z_2}{\mathrm{d}R_2}\sin\tau\\&+p_1\cot\Sigma-C=0.\end{aligned} \tag{22}$$

Once obtained τ will serve to calculate rotor coordinates after the manufacturing process. The obtained rotor coordinates will contain all manufacturing imperfections, like mismatch of the rotor-tool centre distance, error in the rotor-tool shaft angle, axial shift of the tool or tool deformation during the process as they are imposed to the calculation process. A full account of this useful procedure is given by Stosic (1998).

The theory of profiling rotor manufacturing tools presented in this study is equally valid for the main and gate rotors. A typical tool-rotor engagement is presented in Fig. 12 for the main rotor.

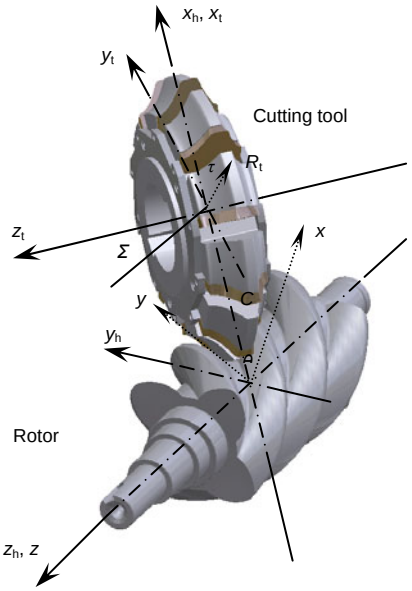

Fig. 12 Rotor (x_h,y_h,z_h) and tool (x_t,y_t,z_t) coordinate systems

5.3 Quantification of manufacturing imperfections

A rotor-tool transformation is used here for a milling tool profile generation. A reverse procedure is used to calculate the 'manufactured' rotors. The rack generated 5–6 rotors with an out diameter of 128 mm described by Stosic (1998) are used as given profiles: $x(t)$ and $y(t)$. Then a tool-rotor transformation is used to quantify the influence of manufacturing imperfections upon the quality of the produced rotor profile. Both linear and angular offset were considered.

As shown in Figs. 13 and 14, the rotors, main manufactured with the shaft angle offset of 0.1° and gate with the centre distance offset of 50 μm are compared with the original rotors. The rotors manufactured with imperfections, main with the tool axial offset of 50 μm and gate with the certain tool body deformation, resulted in a relative motion angle θ offset of 0.1°. More information is given in Stosic (2006).

5.4 Compensation of tool wear

Tool wear is inevitable in any machining process. Following Stosic (2006), where a geometric study of tool wear was performed, it can be shown that tool wear is proportional to the relative speed of the tool and the rotor.

The tool wear caused by machining of the typical screw compressor rotors is presented in Fig. 15 with the tool wear and superimposed on the unworn tool profile to demonstrate its distribution. As shown in Fig. 15a, the departure of the manufactured rotors from the theoretical ones is not uniform, and it is larger at the regions where the relative tool to rotor speed is higher.

It is logical to expect that this difference can be compensated by adjusting the tool setting in the machine. Indeed, if the tool to rotor centre distance and the angle between the rotor and tool shafts are adjusted to depart from their theoretical values, a better match of the manufactured and theoretical rotors may be achieved. The result of such a procedure is presented in Fig. 15b.

By comparison, the effect of the tool wear is reduced at least twofold if compensation is applied (Fig. 15). This means that the tool operating life may be more than doubled before dressing or sharpening is required if its wear is compensated by the adjustment of the tool setting parameters.

6 Conclusions

Although the screw compressor is now a well developed product, greater involvement of engineering science in the form of computer modeling and mathematical analysis at the design stage, makes further improvements in efficiency and reduction in

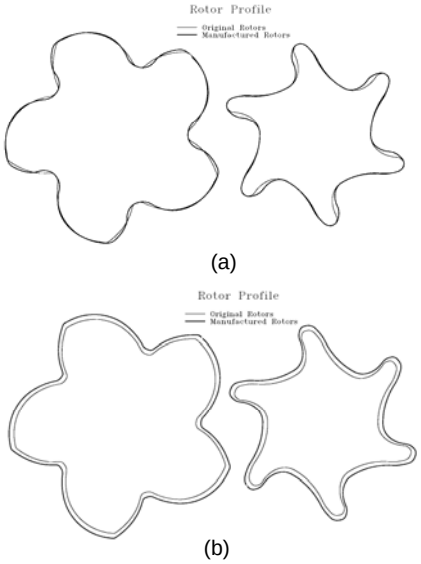

Fig. 13 Effect of an error of 0.1° in the tool-rotor shaft angle (a) and effect of an error of 50 μm in the tool-rotor centre distance (b)

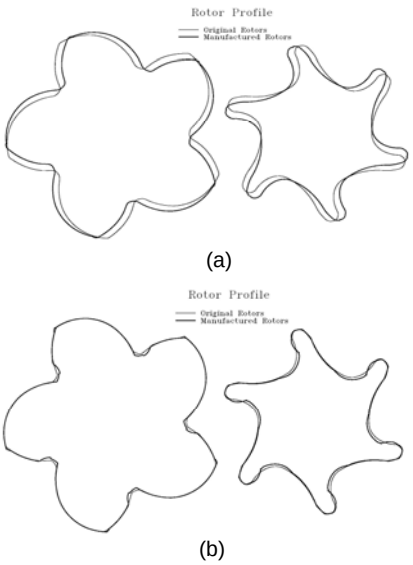

Fig. 14 Effect of an error of 50 μm in the axial tool position (a) and effect of a mismatch of 0.1° in the meshing angle due to the tool deformation (b)

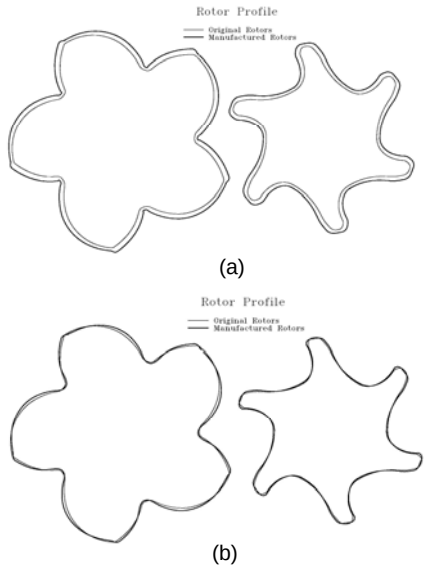

Fig. 15 Effect of tool wear (a) and tool wear compensation (b)
The original rotors is machined by the unworn tool, and departure of the rotors manufactured by the worn tool is corrected by a 50 μm reduction in the centre distance and a 0.1° variation in shaft angle

size and cost possible. Despite the advanced stage of modern rotor profile generation, there is still scope for new methods or procedures to improve them further and to produce stronger but lighter rotors with higher displacement and lower contact stress. The procedures described in this paper serve as a basis for employment of design software used for the development of screw machines. It requires only few input parameters, which specify geometry and operating conditions of a screw compressor.

References

Amosov, P.E., Bobrikov, N.I., Svarc, I.I., Vernii, A.L., 1977. Vintovie Kompresornie Mashinii Spravochnik (Screw Compression Machines-Handbook). Mashinstroienie, Leningrad (in Russian).

Andreev, P.A., 1961. Vintovie Kompressornie Mashinii (Screw Compression Machines-Handbook). Sudprom, Leninngrad (in Russian).

Astberg, A., 1982. Patent Rotary Positive Displacement Fluid Machines. GB Patent 2092676B.

Bammert, K., 1979. Rotating Piston Machine with Parallel Meshing Rotors. DE Patent 2911415 (in German).

Chen, C.H., 1995. Screw Compressor with Rotors Having Hyper Profile. US Patent 5454701.

Fleming, J.S., Tang, Y., Cook, G., 1998. The twin helical screw compressor, Part 1: Development, applications and competetive position. *Journal of Mechanical Engineering Science*, **212**:355.

Holmes, C.S., Stephen, A.C., 1999. Flexible Profile Grinding of Screw Compressor Rotors. International Conference on Compressors and Their Systems, IMechE, London, p.126.

Hough, D., Morris, S.J., 1984. Screw Rotor Machines. GB Patent 2159883A.

Lee, H.T., 1988. Screw-Rotor Machine with an Ellipse as a Part of its Male Rotor. US Patent 4890992.

Lysholm, A., 1942. A new rotary compressor. *Proceeding of the Institution of Mechanical Engineers*, **150**:11.

Lysholm, A., 1967. Screw Rotor Machine. US Patent 3314598.

Menssen, E., 1977. Screw Compressor with Involute Profiled Teeth. US Patent 4028026.

Rinder, L., 1987. Screw Rotor Profile and Method for Generating. US Patent 4643654.

Robert, N., 1952. Helical Rotary Engine. US Patent 2622787.

Shibbye, C.B., 1979. Screw-Rotor Machine with Straight Flank Sections. US Patent 4140445.

Stosic, N., 1996a. Plural Screw Positive Displacement Machines. EP Patent 898655.

Stosic, N., 1996b. Plural Screw Positive Displacement Machines. GB Patent 9610289.2.

Stosic, N., 1996c. Plural Screw Positive Displacement Machines. US Patent 6296461.

Stosic, N., 1996d. Plural Screw Positive Displacement Machines. WO Patent 9743550.

Stosic, N., 1998. On gearing of helical screw compressor rotors. *Journal of Mechanical Engineering Science*, **212**:587.

Stosic, N., 2005. Identification of Constraints in the Optimal Generation of Screw Compressor Rotors by the Pressure Angle Method. Proceedings of International Conference on Compressors and their Systems, IMechE, London, p.33.

Stosic, N., 2006. A geometric approach to calculating tool wear in screw rotor machining. *International Journal of Machine Tools and Manufacture*, **46**(15):1961-1965. [doi:10.1016/j.ijmachtools.2006.01.012]

Stosic, N., Hanjalic, K., 1997. Development and optimization of screw machines with a simulation model, part I: profile generation. *Journal of Fluids Engineering*, **119**(3):659. [doi:10.1115/1.2819295]

Stosic, N., Smith, I.K., Kovacevic, A., 2003. Optimisation of screw compressors. *Journal of Applied Thermal Engineering*, **23**(10):1177. [doi:10.1016/S1359-4311(03)00059-0]

Stosic, N., Smith, I.K., Kovacevic, A., 2005. Screw Compressors: Mathematical Modeling and Performance Calculation. Springer Verlag, Berlin, Germany.

Stosic, N., Mujic, E., Smith, I.K., Kovacevic, A., 2008. Profiling of Screw Compressor Rotors by Use of Direct Digital Simulation. 19th International Compressor Engineering Conference, Lafayette, Indiana, USA.

Tang, Y., Fleming, J.S., 1994. Clearances between the rotors of helical screw compressors: their determination, optimization and thermodynamic consequences. *Journal of Process Mechanical Engineering*, **208**:155.

Xing, Z.W., 2000. Screw Compressors: Theory, Design and Application. China Machine Press, Beijing, China (in Chinese).